TTP14-018
LPSC-14-130

Vacuum stability of the effective Higgs potential in the Minimal Supersymmetric Standard Model

Markus Bobrowski,[1,*] Guillaume Chalons,[1,2,†] Wolfgang G. Hollik,[1,‡] and Ulrich Nierste[1,§]

[1] *Institut für Theoretische Teilchenphysik, Karlsruhe Institute of Technology, Engesserstraße 7, 76128 Karlsruhe, Germany*
[2] *Laboratoire de Physique Subatomique et de Cosmologie, Université Grenoble-Alpes, CNRS/IN2P3, 53 Avenue des Martyrs, F-38026 Grenoble, France*

The parameters of the Higgs potential of the Minimal Supersymmetric Standard Model (MSSM) receive large radiative corrections which lift the mass of the lightest Higgs boson to the measured value of 126 GeV. Depending on the MSSM parameters, these radiative corrections may also lead to the situation that the local minimum corresponding to the electroweak vacuum state is not the global minimum of the Higgs potential. We analyze the stability of the vacuum for the case of heavy squark masses as favored by current LHC data. To this end we first consider an effective Lagrangian obtained by integrating out the heavy squarks and then study the MSSM one-loop effective potential V_{eff}, which comprises all higher-dimensional Higgs couplings of the effective Lagrangian. We find that only the second method gives correct results and argue that the criterion of vacuum stability should be included in phenomenological analyses of the allowed MSSM parameter space. Discussing the cases of squark masses of 1 and 2 TeV we show that the criterion of vacuum stability excludes a portion of the MSSM parameter space in which $|\mu \tan\beta|$ and $|A_{\text{t}}|$ are large.

PACS numbers: 12.60.Jv, 14.80.Da

I. INTRODUCTION

The Higgs sector of the Minimal Supersymmetric Standard Model (MSSM) comprises two Higgs doublets H_{u} and H_{d} with tree-level Yukawa couplings to up-type and down-type fermions, respectively. Their self-interaction is described by a special version of the Higgs potential of a two-Higgs-doublet model (2HDM) [? ?]:

$$\begin{aligned} V = {} & m_{11}^2\, H_{\text{d}}^\dagger H_{\text{d}} + m_{22}^2\, H_{\text{u}}^\dagger H_{\text{u}} + \left(m_{12}^2\, H_{\text{u}} \cdot H_{\text{d}} + \text{h.c.}\right) \\ & + \frac{\lambda_1}{2}\left(H_{\text{d}}^\dagger H_{\text{d}}\right)^2 + \frac{\lambda_2}{2}\left(H_{\text{u}}^\dagger H_{\text{u}}\right)^2 + \lambda_3\left(H_{\text{u}}^\dagger H_{\text{u}}\right)\left(H_{\text{d}}^\dagger H_{\text{d}}\right) \\ & + \lambda_4\left(H_{\text{u}}^\dagger H_{\text{d}}\right)\left(H_{\text{d}}^\dagger H_{\text{u}}\right) + \Bigg(\frac{\lambda_5}{2}\left(H_{\text{u}} \cdot H_{\text{d}}\right)^2 \\ & - \lambda_6\left(H_{\text{d}}^\dagger H_{\text{d}}\right)\left(H_{\text{u}} \cdot H_{\text{d}}\right) - \lambda_7\left(H_{\text{u}}^\dagger H_{\text{u}}\right)\left(H_{\text{u}} \cdot H_{\text{d}}\right) + \text{h.c.}\Bigg). \end{aligned} \tag{1}$$

The neutral components of $H_{\text{u,d}}$ acquire vacuum expectation values (vevs) $v_{\text{u,d}}/\sqrt{2}$ satisfying $\sqrt{v_{\text{u}}^2 + v_{\text{d}}^2} = v \simeq 246\,\text{GeV}$. In the MSSM the tree-level values for the self-couplings $\lambda_{1\ldots4}$ are fixed in terms of small gauge couplings and those of $\lambda_{5\ldots7}$ vanish altogether. As a consequence, the mass of the lightest Higgs boson h^0 cannot exceed the Z-boson mass at tree level. Radiative corrections can lift m_{h^0} well above m_Z [?] and must indeed be large, if the discovered Higgs boson with a mass of 125 GeV [? ?] is identified with h^0. The largest radiative corrections to m_{h^0} involve the top Yukawa coupling Y_{t} and stem from loop diagrams with stops or tops. Diagrammatic two-loop [? ? ? ?] and three-loop [? ?] corrections to m_{h^0} are implemented in the public computer programs `FeynHiggs` [? ? ? ? ?] and `H3m` [?], respectively. No stops at the LHC have been found, suggesting that the masses $m_{\tilde{t}_{1,2}}$ of the two stop eigenstates are well above the electroweak scale v. Heavy stops require large values for the bilinear supersymmetry-breaking terms $m_{\tilde{t}_{\text{L,R}}}^2$, which are the diagonal elements of the stop mass matrix. In the limit $m_{\tilde{t}_{\text{L,R}}}^2 \gg v$ one can integrate out the heavy stops to find an effective 2HDM Lagrangian $\mathcal{L}_{\text{2HDM}} \supset -V$, which encodes the stop effects in terms of effective parameters m_{ij}^2 and λ_i. To derive V one must calculate diagrams with two or four external Higgs lines and a stop loop. The λ_i receive shifts proportional to Y_{t}^4 which are crucial to lift m_{h^0} to the measured value. If $\tan\beta = v_{\text{u}}/v_{\text{d}}$ (or the trilinear supersymmetry-breaking term A_{b}) is large, also sbottom loops must be considered. An exhaustive analysis, matching the MSSM with heavy superpartners onto a 2HDM at the full one-loop level can be found in [?]. Denoting the masses of the top and bottom squarks generically with $M_{\tilde{q}}$, the Higgs masses and couplings calculated from the effective 2HDM reproduce the results of the diagrammatic calculation as an expansion in $1/M_{\tilde{q}}^2$. The accuracy of this expansion can be improved by adding terms of higher dimension to (1) obtained from loop diagrams with more external legs as shown in Fig. 1. Effective Lagrangians permit the resummation of large logarithms $\ln(M_{\tilde{q}}/v)$ to all orders in perturbation theory by solving the renormalization-group (RG) equations for the parameters. Note that the top quark is not integrated out, $\mathcal{L}_{\text{2HDM}}$ contains the full field content of the 2HDM and *e.g.* top-loop contributions to the Higgs mass matrix are calculated from $\mathcal{L}_{\text{2HDM}}$.

The effective 2HDM lagrangian reproduces the low-

* markus.bobrowski@kit.edu
† chalons@lpsc.in2p3.fr
‡ wolfgang.hollik@kit.edu
§ ulrich.nierste@kit.edu

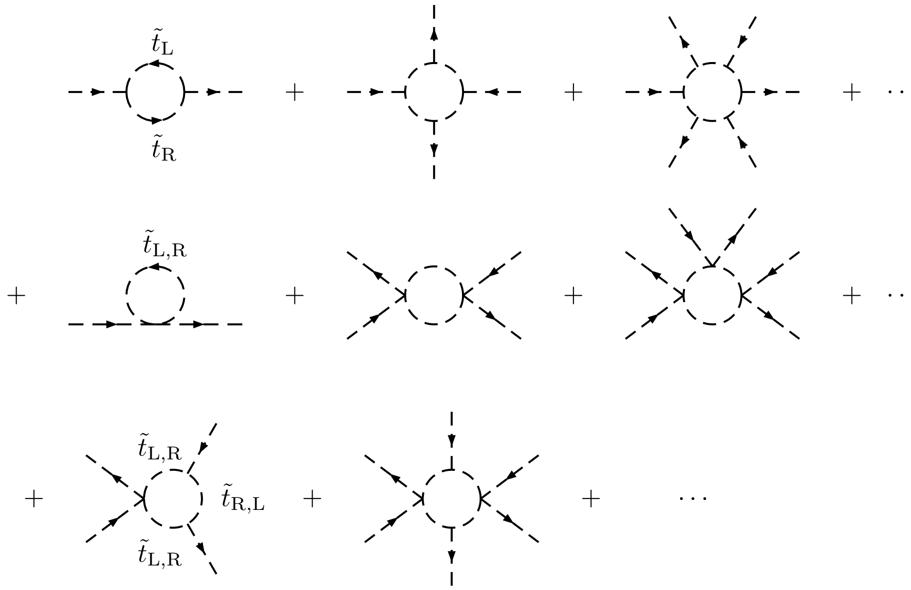

FIG. 1. The 1-loop contribution to the effective potential as the sum of all one-particle irreducible diagrams with zero external momenta.

energy ($E \ll M_{\tilde{q}}$) phenomenology of the MSSM for the case $v, m_{h^0}, m_{A^0}, m_{H^0}, m_{H^\pm} \ll M_{\tilde{q}}$. The Yukawa sector of $\mathcal{L}_{\mathrm{2HDM}}$ has been widely studied [? ? ? ? ? ? ? ? ? ? ? ? ? ? ? ? ? ? ?], while little attention has been devoted to the Higgs self-interaction in V. Instead, effective-Lagrangian studies (typically addressing calculations of m_{h^0}) have used a Higgs potential with a single Higgs doublet, describing instead the hierarchy $v, m_{h^0} \ll m_{A^0}, m_{H^0}, m_{H^\pm}, M_{\tilde{q}}$, *i.e.* integrating out the heavy non-standard Higgs fields at the same scale as the heavy superpartners [? ?]. In [?] the diagrammatic two-loop result for m_{h^0} of [?] is complemented with the leading and next-to-leading logarithms $\ln(M_{\tilde{q}}/v)$ of higher orders found from the RG analysis of the single-Higgs-doublet Lagrangian in [? ?]. The corresponding result is implemented in the current version `2.10.0` of `FeynHiggs`. Other public computer codes incorporating two-loop accuracy for the Higgs boson mass are `Softsusy` [?], `SuSpect` [?] and `SPheno` [?].

Depending on the values of the λ_i the 2HDM potential in (1) may be unbounded from below (UFB) or may develop an unwanted global minimum rendering “our” vacuum state with $v = 246\,\mathrm{GeV}$ unstable. The parameter ranges complying with vacuum stability have been identified in [? ?] and the corresponding constraints on m_{ij}^2 and λ_i are routinely included in phenomenological analyses of 2HDM (see *e.g.* [? ? ? ?]). These vacuum stability constraints can also be imposed on the effective $\mathcal{L}_{\mathrm{2HDM}}$ obtained from the MSSM by integrating out heavy squarks. In this paper we show that there are indeed ranges for the MSSM parameters for which V in (1) is unbounded from below. However, when V drops below its local minimum with $v = 246\,\mathrm{GeV}$ the Higgs fields are so large that the higher-dimensional corrections to V depicted in Fig. 1 become important. All these contributions can be resummed and constitute a piece of the effective Coleman-Weinberg potential [?]. In [? ? ?] the multiple minima of the full tree-level scalar potential have been surveyed in great detail and strong constraints on their existence were derived. Analyses allowing the electroweak vacuum to be metastable, with a lifetime exceeding the age of the universe, have been performed in [? ? ? ? ? ?]. While the effective Higgs potential for the MSSM has been widely studied [? ? ? ? ? ? ? ? ? ? ? ? ?] with focus on Higgs masses, the criterion of vacuum stability of the loop-corrected Higgs potential has previously not been applied to constrain the MSSM parameter space. The studies performed in [? ? ?] used the `Vevacious` code to exploit the vacuum stability constraint on the parameter space. This code makes use of the effective Coleman-Weinberg potential but only in the vicinity of all the vacua found by minimization of the *tree-level* scalar potential. However, this procedure does not guarantee to find minima induced purely by radiative effects [?], which is precisely the topic we analyze in this paper.

This paper is organized as follows: In Sec. II we rederive the effective potential of the MSSM and discuss some of its properties. In Sec. III we illustrate the main result of this paper, a novel constraint on the MSSM parameter space from the requirement of vacuum stability. Finally we conclude.

II. EFFECTIVE LAGRANGIAN AND EFFECTIVE POTENTIAL

Once we integrate out the heavy top and bottom squarks we find the *effective Lagrangian*

$$\mathcal{L}_{\rm 2HDM}^{\rm Higgs} = \mathcal{L}_{\rm kin} - V + \mathcal{L}_{\rm der,D\geq 6} - V_{D\geq 6} \qquad (2)$$

with the kinetic term $\mathcal{L}_{\rm kin}$, the Higgs potential V of (1), and the contribution from higher-dimensional operators $\mathcal{L}_{\rm der,D\geq 6} - V_{D\geq 6}$. The former term $\mathcal{L}_{\rm der,D\geq 6}$ contains operators of dimension 6 and higher with at least two derivatives acting on the Higgs fields. One effect of $\mathcal{L}_{\rm der,D\geq 6}$ are contributions suppressed by one or more powers of $1/M_{\tilde{q}}^2$ to the field renormalization constants of the physical Higgs fields. (These renormalization constants can be matrices, permitting kinetic mixing of different Higgs fields.) This effect matters for the expression of the doublet components in terms of physical fields, but is of no relevance for the discussion of global properties of the Higgs potential in this paper. Other ingredients of $\mathcal{L}_{\rm der,D\geq 6}$ are derivative couplings and couplings to gauge fields, which are also irrelevant for our analysis. The Higgs potential $V + V_{D\geq 6}$ contains the usual bilinear and quadrilinear tree-level contributions and the loop contributions depicted in Fig. 1. If the effective Lagrangian is used to calculate Higgs masses and mixing angles, the series of higher-dimensional terms in $\mathcal{L}_{\rm 2HDM}$ will give corrections which quickly decrease with powers of $1/M_{\tilde{q}}^2$.

Our purpose, however, is to study global properties of $V + V_{D\geq 6}$ and $V_{D\geq 6}$ can be sizable in the range of large Higgs field amplitudes. It is well-known how to resum the contributions with $D = 6, 8, 10\ldots$, the result is the squark contribution to the *effective potential*. The concept of the effective potential does not require a mass hierarchy between the particles running in the loop and the external Higgs bosons and indeed the original application of Coleman and Weinberg [?] involves a massless field in the loop. The focus of [?] is the generation of a small dynamical Higgs mass in a theory with zero tree-level mass through spontaneous symmetry breaking induced by quantum effects, which are subsumed in the effective potential. Instead the scope of our paper is the destabilization of the tree-level MSSM Higgs potential by very heavy particles (top and bottom squarks). Still, as in the original paper we use the effective potential to "survey all possible vacua simultaneously" [?].

In Sec. II A we calculate the higher-dimensional couplings of neutral Higgs bosons in $V_{D\geq 6}$. In Sec. II B we summarize some of the conceptual aspects of the effective potential and show that the one-loop effective potential of the MSSM [?] indeed reproduces the couplings derived in Sec. II A correctly.

A. Effective 2HDM Lagrangian

The two SU(2) doublet Higgs fields of the MSSM are

$$H_{\rm u} = \begin{pmatrix} h_{\rm u}^+ \\ h_{\rm u}^0 \end{pmatrix}, \qquad H_{\rm d} = \begin{pmatrix} h_{\rm d}^0 \\ -h_{\rm d}^- \end{pmatrix} \qquad (3)$$

with hypercharges $+1/2$ and $-1/2$, respectively, and vevs $\langle h_{\rm u}^0 \rangle = v_{\rm u}/\sqrt{2}$ and $\langle h_{\rm d}^0 \rangle = v_{\rm d}/\sqrt{2}$. As usual we define their ratio as $\tan\beta = v_{\rm u}/v_{\rm d}$. The most general renormalizable Higgs potential V of an arbitrary 2HDM [? ?] is given in (1) above, where $a \cdot b = a^{\rm T}\,\epsilon\, b$ and ϵ denotes the totally antisymmetric tensor with $\epsilon_{12} = +1$. At tree-level, V is unambiguously determined by F- and D-terms and the soft supersymmetry breaking Lagrangian:

$$\begin{aligned} m_{11}^{2\,\rm tree} &= |\mu|^2 + m_{H_{\rm d}}^2, & \lambda_{1,2}^{\rm tree} &= -\lambda_3^{\rm tree} = \frac{g^2 + g'^2}{4}, \\ m_{22}^{2\,\rm tree} &= |\mu|^2 + m_{H_{\rm u}}^2, & \lambda_4^{\rm tree} &= \frac{g^2}{2}, \\ m_{12}^{2\,\rm tree} &= B_\mu, & \lambda_5^{\rm tree} &= \lambda_6^{\rm tree} = \lambda_7^{\rm tree} = 0. \end{aligned} \qquad (4)$$

With the minimization conditions one can eliminate m_{11}^2 and m_{22}^2 in terms of v and β. At tree-level, these relations read

$$\begin{aligned} m_{11}^{2\,\rm tree} &= m_{12}^{2\,\rm tree} \tan\beta - \frac{v^2}{2}\cos(2\beta)\lambda_1^{\rm tree}, \\ m_{22}^{2\,\rm tree} &= m_{12}^{2\,\rm tree} \cot\beta + \frac{v^2}{2}\cos(2\beta)\lambda_1^{\rm tree}. \end{aligned} \qquad (5)$$

One further has the relation $2m_{12}^{2\,\rm tree} = m_A^{2\,\rm tree}\sin(2\beta)$, where $m_A^{\rm tree}$ is the tree approximation to the mass of the pseudoscalar Higgs boson A^0. This relation and those in (5) change once radiative corrections are included, *e.g.* the formulae are affected by loop corrections to $\lambda_{1\ldots3,\,5\ldots7}$ (see eqs. (23)–(27) of [?]) and the parameters of $V_{D\geq 6}$. For the following discussion it is useful to write

$$\left(V + V_{D\geq 6}\right)\Big|_{h_{u,d}^{\pm}\to 0} = V_0 + V_1, \qquad (6)$$

where V_0 and V_1 denote the tree and one-loop contributions, respectively, and the subscript on the LHS means that the charged Higgs fields are set to zero. V_0 equals V with the parameters in (4), while V_1 is obtained from the sum of one-loop diagrams in Fig. 1. Neglecting loops with small gauge couplings (which are kept in the tree-level terms) and retaining only the stop loop for the moment the result has the schematic form

$$V_1 = -\sum_{k=0}^{\infty}\sum_{n=0}^{\infty} a_{kn}\left(h^\dagger h\right)^k \left(h_{\rm u}^{0\dagger} h_{\rm u}^0\right)^n. \qquad (7)$$

Here $h = h_{\rm d}^{0\dagger} - h_{\rm u}^0 A_{\rm t}/(\mu^* Y_{\rm t})$ is the linear combination of neutral Higgs fields coupling to the stop loop (see Fig. 2) and a_{kn} is calculated from one-particle irreducible one-

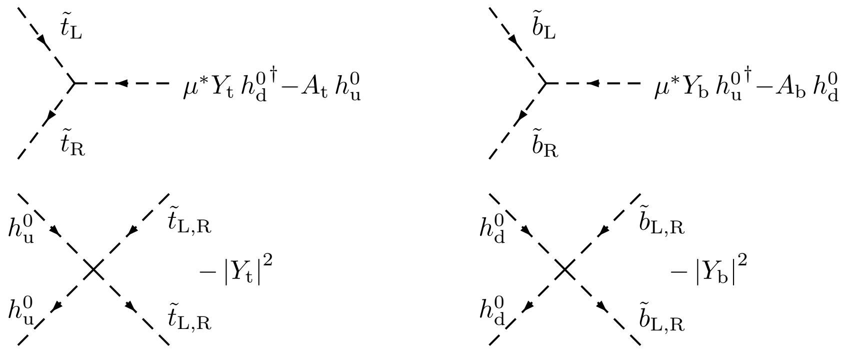

FIG. 2. Couplings of neutral Higgs fields to squarks in the MSSM. μ is the higgsino mass parameter and $Y_\mathrm{t,b}$ and $A_\mathrm{t,b}$ are the Yukawa coupling and trilinear SUSY-breaking term, respectively, of top or bottom (s)quarks.

loop diagrams with $2k+2n$ legs; k denotes the number of $\tilde{t}_\mathrm{R}^*$-$\tilde{t}_\mathrm{L}$-h vertices (and equally many $\tilde{t}_\mathrm{L}^*$-$\tilde{t}_\mathrm{R}$-$h^\dagger$ vertices) and n is the number of $\tilde{t}_\mathrm{L/R}^*$-$\tilde{t}_\mathrm{L/R}$-$h_\mathrm{u}^{0\dagger}$-h_u^0 vertices. We only considered field configurations with $h_\mathrm{u}^+ = h_\mathrm{d}^- = 0$. Relaxing this constraint might exclude additional parts of the MSSM parameter space (corresponding to charge-breaking minima), but according to [**?**], such minima play no significant role for the analysis. The sbottom contribution (relevant only for large $\tan\beta$ or large A_b) adds to (7) an analogous term with h representing a different linear combination of $h_\mathrm{u}^\dagger$ and h_d and h_u^0 replaced by h_d^0. The coefficients a_{kn} read

$$
\begin{aligned}
a_{kn} =& |\mu|^{2k}|Y_\mathrm{t}|^{2n+2k}\,\frac{1}{k}\sum_{j=0}^{n}\frac{(j+k-1)!}{j!(k-1)!}\frac{(n-j+k-1)!}{(n-j)!(k-1)!}\,I_{k+j,k+n-j}(M_{\tilde{Q}}^2, M_{\tilde{\mathrm{t}}}^2) \text{ for } n,k\geq 1,\\
a_{k0} =& |\mu Y_\mathrm{t}|^{2k}\,\frac{1}{k}\,I_{k,k}(M_{\tilde{Q}}^2, M_{\tilde{\mathrm{t}}}^2) \text{ for } k\geq 1,\\
a_{0n} =& |Y_\mathrm{t}|^{2n}\frac{1}{n}\left[I_{n,0}(M_{\tilde{Q}}^2) + I_{0,n}(M_{\tilde{\mathrm{t}}}^2)\right] \text{ for } n\geq 1.
\end{aligned}
\tag{8}
$$

Here $I_{p,q}(M_{\tilde{Q}}^2, M_{\tilde{\mathrm{t}}}^2)$ is the result of the one-loop diagram with p propagators of $\tilde{t}_\mathrm{L}$ and q propagators of $\tilde{t}_\mathrm{R}$:

$$
\begin{aligned}
I_{p,q}(M_{\tilde{Q}}^2, M_{\tilde{\mathrm{t}}}^2) =& \frac{3}{16\pi^2}\frac{1}{(p-1)!(q-1)!}\times\\
& \frac{\partial^{p-1}}{\partial(M_{\tilde{Q}}^2)^{p-1}}\frac{\partial^{q-1}}{\partial(M_{\tilde{\mathrm{t}}}^2)^{q-1}}\frac{A_0(M_{\tilde{Q}}^2)-A_0(M_{\tilde{\mathrm{t}}}^2)}{M_{\tilde{Q}}^2-M_{\tilde{\mathrm{t}}}^2}\\
& \text{for } q,p\geq 1,\\
I_{n,0}(M^2) =& \frac{3}{16\pi^2}\frac{1}{(n-1)!}\frac{\partial^{n-1}}{\partial(M^2)^{n-1}}A_0(M^2)\\
& \text{for } n\geq 1,\\
I_{0,n}(M^2) =& I_{n,0}(M^2).
\end{aligned}
\tag{9}
$$

In this equation $I_{p,q}$ is expressed in terms of derivatives of the tadpole function, which equals $A_0(M^2) = M^2(1-\ln(M^2/Q^2))$ when evaluated at the scale Q in the $\overline{\mathrm{MS}}/\overline{\mathrm{DR}}$ scheme. The derivation of a_{k0} and a_{0n} is straightforward, the calculation of the combinatorial factors can be found in standard textbooks. To understand a_{kn} for the case with both non-zero k and n, consider first a diagram with $k\neq 0$ and $n=0$, depicted in the first row of Fig. 1. There are $k!(k-1)!$ diagrams (giving identical results for zero external momenta). After dividing off the combinatorial factor $(k!)^2$ associated with the field monomial in (7), one verifies the factor of $1/k$ in (8). These loops with only 3-point vertices have k propagators of $\tilde{t}_\mathrm{L}$ and equally many propagators of $\tilde{t}_\mathrm{R}$. Starting from such a loop we now attach n four-point vertices to the diagram, *i.e.* we pass from the first to the third row in Fig. 1. The sum in (8) takes care of the possibilities to place j four-point vertices on a $\tilde{t}_\mathrm{L}$ line and $n-j$ such vertices on a $\tilde{t}_\mathrm{R}$ line. There are $(j+k-1)!/(j!(k-1)!)$ possibilities for the j placements on a $\tilde{t}_\mathrm{L}$ line, and $(n-j+k-1)!/((n-j)!(k-1)!)$ ways to place the remaining $n-j$ vertices. (These factors correspond to a standard exercise of combinatorics and count the number of orderless configurations with repetitions of j balls having k possible colors.) Finally there are $(n!)^2$ ways to connect the added 4-point vertices with the external h_u^0 and h_u^{0*} fields, which matches the combinatorial factor of the field monomial in (7).

The calculation of a_{kn} and the resummation can be elegantly done with techniques developed in the effective potential approach used in Sec. II B. We nevertheless find it instructive to calculate a_{kn} explicitly as described above and to verify that the effective-potential method reproduces the result correctly.

B. Effective potential

To resum the series in (7) one defines particle masses which depend on the Higgs fields of the theory. We need the stop mass matrix

$$\mathcal{M}^2_{\tilde{\mathrm{t}}} = \begin{pmatrix} M^2_{\tilde{Q}} + \left|Y_\mathrm{t}\, h^0_\mathrm{u}\right|^2 & -\mu^* Y_\mathrm{t}\, h^{0\,\dagger}_\mathrm{d} + A_\mathrm{t}\, h^0_\mathrm{u} \\ -\mu Y^*_\mathrm{t}\, h^0_\mathrm{d} + A^*_\mathrm{t}\, h^{0\,\dagger}_\mathrm{u} & M^2_{\tilde{\mathrm{t}}} + \left|Y_\mathrm{t}\, h^0_\mathrm{u}\right|^2 \end{pmatrix}, \quad (10)$$

where $M^2_{\tilde{Q}}$ and $M^2_{\tilde{\mathrm{t}}}$ are the bilinear soft supersymmetry-breaking terms for $\tilde{Q} = (\tilde{t}, \tilde{b})$ and $\tilde{t}_\mathrm{R}$, respectively. We have neglected D-term contributions, which are suppressed by gauge couplings.

A convenient way to perform the summation is to solve

$$G_1 = -\mathrm{i}\, \frac{\partial}{\partial h} V_1, \quad (11)$$

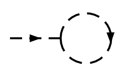

where G_1 is the Green function of the depicted h tadpole with field-dependent stop mass eigenstates propagating in the loop, with h defined after (7) [?]. Integrating (11) w.r.t. h fixes the stop loop contribution $V_1^{\tilde{t}}$ to V_1 up to an arbitrary function of h^0_u. The correct dependence on h^0_u is then found by deriving $V_1^{\tilde{t}}$ w.r.t. h^0_u and $h^{0\dagger}_\mathrm{u}$ and comparing the result with the h^0_u-$h^{0\dagger}_\mathrm{u}$ two-point function depicted in the second row of Fig. 1. An alternative way to obtain the missing h^0_u-dependent piece, which leads to exactly the same result, uses the replacement h^0_u by $h^0_\mathrm{u} - w_\mathrm{u}$. In the shifted theory this generates a three point vertex $\tilde{t}^*_{\mathrm{L/R}}$-$\tilde{t}_{\mathrm{L/R}}$-$h^0_\mathrm{u}$ (and its complex conjugate) generating in turn a tadpole diagram. The final result is found after integration over w_u and setting back $w_\mathrm{u} = 0$. We find:

$$\begin{aligned} V_1^{\tilde{t}} = &\frac{3\widetilde{M}^4_\mathrm{t}}{32\pi^2}\Big[(1 + x_\mathrm{t} + y_\mathrm{t})^2 \ln(1 + x_\mathrm{t} + y_\mathrm{t}) \\ &+ (1 - x_\mathrm{t} + y_\mathrm{t})^2 \ln(1 - x_\mathrm{t} + y_\mathrm{t}) \\ &- \left(x^2_\mathrm{t} + y^2_\mathrm{t} + 2y_\mathrm{t}\right)\left(3 - 2\ln\left(\widetilde{M}^2_\mathrm{t}/Q^2\right)\right)\Big], \end{aligned} \quad (12)$$

where the loops have been renormalized in the $\overline{\mathrm{MS}}/\overline{\mathrm{DR}}$ scheme at the scale Q. In (12) we have used the mean soft mass square $\widetilde{M}^2_\mathrm{t} \equiv (M^2_{\tilde{Q}} + M^2_{\tilde{\mathrm{t}}})/2$ and the dimensionless quantities x_t and y_t

$$\begin{aligned} x^2_\mathrm{t} &= \frac{\left|A_\mathrm{t} h^0_\mathrm{u} - \mu^* Y_\mathrm{t} h^{0\,*}_\mathrm{d}\right|^2}{\widetilde{M}^4_\mathrm{t}} + \frac{(M^2_{\tilde{Q}} - M^2_{\tilde{\mathrm{t}}})^2}{4\widetilde{M}^4_\mathrm{t}}, \\ y_\mathrm{t} &= \frac{\left|Y_\mathrm{t} h^0_\mathrm{u}\right|^2}{\widetilde{M}^2_\mathrm{t}}. \end{aligned} \quad (13)$$

An analogous expression (with obvious modifications) is found for the sbottom contribution $V_1^{\tilde{b}}$ and is given below. The shape of $V_1^{\tilde{t}}$ depends solely on the dimensionless parameters x_t and y_t. The summation in (7) converges if $|x_\mathrm{t} \pm y_\mathrm{t}| < 1$. The points $\pm x_\mathrm{t} - y_\mathrm{t} = 1$ are branch points of the logarithm in the closed result (12), which is the analytic continuation of the sum beyond the radius of convergence. As we will argue below, the interplay between V_0 and V_1 can lead to a potential with an unstable vacuum.

So far we have strictly argued along the line of deriving an effective Lagrangian and have resummed the higher-dimensional terms in $V_{D\geq 6} \subset \mathcal{L}_{2\mathrm{HDM}}$, which arise from integrating out the heavy squarks. As long as one stays in this framework, one can deny any relevance of V_1 for large $h_{\mathrm{u,d}}$ amplitudes with $|x_\mathrm{t} - y_\mathrm{t}| \geq 1$, because the series in (7) diverges in this domain.

The justification of the use of V_1 for $|x_\mathrm{t} - y_\mathrm{t}| \geq 1$ lies in the effective potential definition of Coleman and Weinberg [?], which furthermore does not require the particles running in the loop to be heavy. We will later add the quark loops to V_1 to get the full one-loop effective potential V_eff in the sense of Coleman and Weinberg. We briefly recall its derivation. Consider a theory with a complex scalar field ϕ. Connected Green functions can be derived by functional variations of a generating functional $W(J)$ w.r.t. a classical source $J(x)$. The classical field ϕ_c is defined as the expectation value of the field operator in the Fock vacuum in the presence of the source J:

$$\phi_\mathrm{c} = \left[\frac{\langle\, 0\,|\,\phi\,|\,0\,\rangle}{\langle\, 0\,|\,0\,\rangle}\right]_J. \quad (14)$$

A Legendre transform brings us to the *effective action* $\Gamma(\phi_\mathrm{c}) := W(J) - \int d^4x J(x)\phi_\mathrm{c}(x)$, which is the generating functional of one-particle irreducible Green functions. The effective potential $V(\phi_\mathrm{c})$ is defined as the first term of an expansion of $\Gamma(\phi_\mathrm{c})$ in terms of derivatives of ϕ_c:

$$\Gamma(\phi_\mathrm{c}) = \int d^4x \left[-V(\phi_\mathrm{c}) + \frac{1}{2}(\partial_\mu \phi_\mathrm{c})^2 Z(\phi_\mathrm{c}) + \ldots\right] \quad (15)$$

Thus the n-th derivative of $V(\phi_\mathrm{c})$ is the sum of all one-particle irreducible graphs with n legs and zero external momenta. $V(\phi_\mathrm{c})$ can be physically interpreted as follows [?]: The effective potential $V(\phi_\mathrm{c})$ is the potential energy density of the classical field in the quantized theory, *viz.* the expectation value of the energy density in the state $|\,0\,\rangle$ that minimizes $\langle\, 0\,|\,H\,|\,0\,\rangle$ subject to (14) (where H is the Hamiltonian density operator). For vanishing sources $J \to 0$, the theory's vacua seek to minimize the potential energy, *i.e.*

$$\frac{\delta V(\phi_c)}{\delta \phi_c} = 0. \tag{16}$$

If this is the case for $\phi_c = \langle \phi \rangle \neq 0$, the field takes a vacuum expectation value of $\langle \phi \rangle$, and internal symmetries are broken spontaneously. If there is no asymmetric vacuum in the classical potential, spontaneous symmetry breaking may even emerge as a pure quantum effect. The ground state of the theory, the state of lowest energy, lives in the global minimum of the effective potential [?]. Vacua minimizing the potential only locally are unstable and can pass into the ground state. Coleman and Weinberg [?] have considered the gauge theory of a single scalar with self-interactions due to a classical potential energy density $V_0(\phi)$. They have found

$$V_{\text{eff}}(\phi_c) = \frac{1}{64\pi^2} \text{Tr}\left[V_0''^2(\phi_c) \ln V_0''(\phi_c)\right] + P(\phi_c), \tag{17}$$

where $P(\phi_c)$ is a polynomial depending on the choice of the renormalization scheme. $V_0''(\phi_c)$ is the field-dependent mass matrix of the field degrees of freedom circulating in the loop, like the one in (10). To consistently include all terms involving Y_t into V_{eff} we must add the top loop, $V_{\text{eff}} = V_1^{\tilde{t}} + V_1^t$ to complement the result in (12) to the full effective potential, with

$$V_1^t = -\frac{3}{16\pi^2} \left|Y_t h_u^0\right|^4 \left[\ln\left(\left|Y_t h_u^0\right|^2 / Q^2\right) - \frac{3}{2}\right] \tag{18}$$

in the $\overline{\text{MS}}/\overline{\text{DR}}$ scheme. The generic formula in (17) (with the trace replaced by the supertrace to include the fermion loops) has been used in [?] to derive V_{eff}, expressed in terms of the eigenvalues of $\mathcal{M}_{\tilde{t}}^2$. In our calculation, integrating the tadpole in (11), we find the same result. The MSSM case involves two Higgs fields h and h_u^0 and thereby goes beyond the original framework in [?]. Theories with several Higgs fields have been studied in [?]. Our situation with both 3-point and 4-point vertices present in the loops in Fig. 1 is quite special and we have seen a benefit in verifying the commonly used formulae for V_{eff} with our explicit calculation at the end of Sec. II A: By deriving $V_1^{\tilde{t}}$ in (12) w.r.t. h and $h_u^{0\dagger}$ one indeed reproduces the coefficients a_{kn} in (8) with the correct combinatorial factors.

In (12) we have given the explicit form of $V_1^{\tilde{t}}$ in terms of h_u^0 and h_d^{0*}, which is more suitable for the global analysis of V_{eff}. While we further generalize $V_1^{\tilde{t}}$ to complex A_t and μ, we neglect the small D-term contributions, which are included in [?]. Adding the contributions from (s)tops and (s)bottoms, the final ($\overline{\text{MS}}/\overline{\text{DR}}$-scheme) result reads

$$\begin{aligned} V_{\text{eff}} &= V_0 + V_1^{\tilde{t}} + V_1^t + V_1^{\tilde{b}} + V_1^b \\ &= m_{11}^{2\,\text{tree}} |h_d^0|^2 + m_{22}^{2\,\text{tree}} |h_u^0|^2 - 2\,\text{Re}\left(m_{12}^{2\,\text{tree}} h_u^0 h_d^0\right) + \frac{g^2+g'^2}{8}\left(|h_d^0|^2 - |h_u^0|^2\right)^2 \\ &\quad + \frac{3\widetilde{M}_t^4}{32\pi^2}\Bigg[(1+x_t+y_t)^2 \ln(1+x_t+y_t) + (1-x_t+y_t)^2 \ln(1-x_t+y_t) \\ &\qquad - \left(x_t^2 + 2y_t\right)\left(3 - 2\ln\left(\widetilde{M}_t^2/Q^2\right)\right) - 2y_t^2 \ln(y_t) \; + \; \{t \leftrightarrow b\}\Bigg] \end{aligned} \tag{19}$$

with $\widetilde{M}_{t,b}^2 = (M_{\tilde{Q}}^2 + M_{\tilde{t},\tilde{b}}^2)/2$ and stop-loop parameters x_t and y_t defined as in (13); similarly, the sbottom-loop parameters are

$$\begin{aligned} x_b^2 &= \frac{\left|A_b h_d^0 - \mu^* Y_b h_u^{0*}\right|^2}{\widetilde{M}_b^4} + \frac{(M_{\tilde{Q}}^2 - M_{\tilde{b}}^2)^2}{4\widetilde{M}_b^4}, \\ y_b &= \frac{\left|Y_b h_d^0\right|^2}{\widetilde{M}_b^2}. \end{aligned} \tag{20}$$

In (19), the quadrilinear couplings at tree-level λ_i^{tree} were replaced according to (4) and the treatment of the bilinear $m_{ij}^{2\,\text{tree}}$ is discussed in the following section. Note, that the λ_4^{tree} term drops out from the neutral Higgs potential.

Apparently, the effective potential in (17) acquires an imaginary part for values of ϕ_c which render an eigenvalue of $V_0''^2(\phi_c)$ negative. In our case of $V_1^{\tilde{t}}$ this happens for $x-y>1$. The imaginary part of V_{eff} must be dropped to keep the Lagrangian hermitian. The physical meaning of the imaginary part is controversial: Weinberg and Wu consider the case of a theory with a single scalar field ϕ and argue that the imaginary part of $V_{\text{eff}}(\phi_c)$ coincides with the decay rate of a particular quantum state $|\eta\rangle$ satisfying $\langle \eta|\phi|\eta\rangle = \phi_c$ [?]. A different viewpoint on the imaginary part is expressed in [?]. We remark that (the principal values of) analytical continuations are ambiguous, *e.g.* replacing $\ln(1-x_t+y_t)$ by $1/2\ln(1-x_t+y_t)^2$ in (12) does not change the series expansion in (7), but relocates the branch cut in a way that V_{eff} stays real for $|1-x_t+y_t|>1$.

III. PHENOMENOLOGY OF THE MSSM VACUUM INSTABILITY

In this section we give explicit examples for MSSM parameters leading to a V_{eff} for which "our" vacuum with $v = 246\,\text{GeV}$ is unstable.

While loop corrections can render the parameters in (1) complex [? ?], we restrict ourselves to the case of real parameters, with a mass matrix that does not mix CP eigenstates. Writing

$$h_{\text{u}}^0 = \frac{1}{\sqrt{2}}\left(v_{\text{u}} + \phi_{\text{u}} + \mathrm{i}\chi_{\text{u}}\right), \qquad h_{\text{d}}^0 = \frac{1}{\sqrt{2}}\left(v_{\text{d}} + \phi_{\text{d}} + \mathrm{i}\chi_{\text{d}}\right), \tag{21}$$

we trade two of the mass parameters in (19) for $v_{u,d}$ in analogy to (5):

$$\begin{aligned} m_{11}^{2\,\text{tree}} &= m_{12}^{2\,\text{tree}}\tan\beta - \frac{v^2}{2}\cos(2\beta)\lambda_1^{\text{tree}} - \frac{1}{v\cos\beta}\,\frac{\delta}{\delta\phi_{\text{d}}}V_1\bigg|_{\substack{\phi_{\text{u, d}}\to 0\\ \chi_{\text{u, d}}\to 0}}, \\ m_{22}^{2\,\text{tree}} &= m_{12}^{2\,\text{tree}}\cot\beta + \frac{v^2}{2}\cos(2\beta)\lambda_1^{\text{tree}} - \frac{1}{v\sin\beta}\,\frac{\delta}{\delta\phi_{\text{u}}}V_1\bigg|_{\substack{\phi_{\text{u, d}}\to 0\\ \chi_{\text{u, d}}\to 0}}. \end{aligned} \tag{22}$$

The Higgs mass matrices are

$$M_{\text{R}\,ij}^2 = \frac{\delta^2 V}{\delta\phi_i\,\delta\phi_j}\bigg|_{\substack{\phi_{\text{u, d}}\to 0\\ \chi_{\text{u, d}}\to 0}}, \qquad M_{\text{I}\,ij}^2 = \frac{\delta^2 V}{\delta\chi_i\,\delta\chi_j}\bigg|_{\substack{\phi_{\text{u, d}}\to 0\\ \chi_{\text{u, d}}\to 0}}. \tag{23}$$

The mass of the pseudoscalar Higgs A^0 is essentially controlled by $m_{12}^{2\,\text{tree}}$ (for not too small $\tan\beta$). The mass of the lightest scalar Higgs h^0 is very sensitive to radiative corrections, and a calculation from the one-loop effective potential through (23) underestimates m_{h^0} by more than 5 GeV. We, accordingly, can safely calculate m_{A^0} from the non-zero eigenvalue of M_{I}^2, but resort to `FeynHiggs 2.10.0` [? ? ? ?] to obtain m_{h^0} including dominant 2- and 3-loop contributions. While the smallness of gauge couplings governing the tree-level result for m_{h^0} makes the need of higher-order corrections obvious, one does not expect large radiative corrections to the height of the second minimum, which involves large parameters (μ, A_{t}, $m_{\tilde{t}_{\text{L, R}}}^2$) already at the leading one-loop order. The different mass scales entering our analysis are close enough that no large logarithms occur making any renormalization-group improvement obsolete. The scale Q entering V_{eff} explicitly and the couplings and mass parameters implicitly is taken at $\widetilde{M}_{\text{t}}$. We are interested in a heavy A^0 (to satisfy the experimental constraints from $A^0 \to \tau\tau$ and $B_s \to \mu^+\mu^-$) in which case the effect of m_{A^0} on the lightest Higgs mass is small. After choosing values for $\mu, M_{\tilde{Q},\tilde{\text{t}},\tilde{\text{b}}}^2, m_{A^0}$, and $\tan\beta$ we adjust A_{t} to fit $m_{h^0} = 126\,\text{GeV}$. Finally we remark that we take the gluino mass heavier than the squark masses. The gluino mass enters the threshold corrections subsumed in the parameter Δ_{b} which appears in the bottom Yukawa coupling as $Y_{\text{b}} = m_{\text{b}}/(v_{\text{d}}(1+\Delta_{\text{b}}))$ [? ? ? ?] and for sufficiently large gluino mass we can neglect Δ_{b}.

The 1-loop effective scalar potential obtained with this setup is illustrated in Figs. 3 and 4 for a sample parameter point complying with all experimental constraints. We find that supersymmetric quantum effects lead to a second, deeper minimum of the Higgs potential. Relative depth and position of the minima depend crucially on the values of $\mu, A_{\text{t,b}}$, and $\tan\beta$. Large values parametrically enhance the effect of the sfermion loops.

Note that the minimum of the 1-loop contribution is always beyond the branch point of one of the logarithms in V_{eff}. For the case depicted in Fig. 3 the electroweak vacuum is unstable and a transition to the ground state is possible due to quantum tunnelling [? ? ? ?]. Semi-classical methods can be applied to estimate the lifetime of the unstable vacuum. If the inferred lifetime exceeds the age of the universe, the instability of the electroweak vacuum does not matter. However, in the case at hand, with the global minimum appearing for field values of less than 700 GeV, the electroweak vacuum is extremely short-lived. Fig. 3 further shows that the loop-corrected 2HDM potential in (1) (corresponding to a truncation of V_{eff} at terms of dimension 4) does not reveal any problems. It is therefore not sufficient to include loop corrections to the 2HDM parameters to analyze the vacuum stability. Including a finite number of higher-dimension terms leads to a Higgs potential which is unbounded from below (UFB), but the correct feature of a potential with a second minimum is only found from the full V_{eff}. This is not surprising, since the second minimum is in the domain beyond the radius of convergence of the series in (7). Lowering μ slightly raises the second minimum and leads to a parameter point passing our criterion, as depicted in Fig. 4. Note that here the UFB criterion applied to a Higgs potential truncated at a finite dimension $2(k+n)$ leads to a premature exclusion of the corresponding MSSM parameter point.

In the region beyond the branch point, V_{eff} in (19) features an imaginary part, which should be dropped

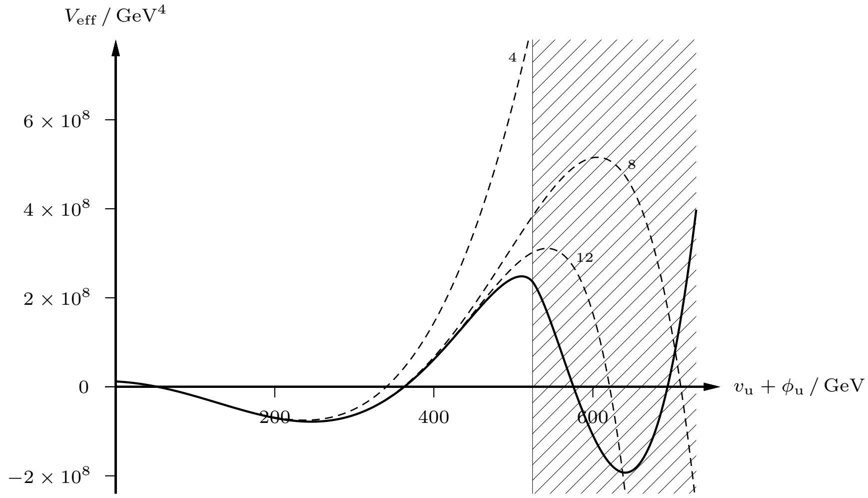

FIG. 3. The 1-loop effective potential $V_{\text{eff}} = V_0 + V_1$ for $\tan\beta = 40$ and $m_{A^0} = 800\,\text{GeV}$. Soft supersymmetry-breaking masses as well as the renormalization scale Q have been taken at 1 TeV. The Higgs couplings in the loops with top and bottom squarks involve $\mu = 2.55\,\text{TeV}$ and $A_{\text{t}} \simeq 1.5\,\text{TeV}$. The hatched area highlights the analytic continuation beyond the branch point at $x - y = 1$. The cases with V_{eff} truncated after terms of dimension $2(k+n) = 4, 8$, and 12 are shown with dashed lines (from top to bottom).

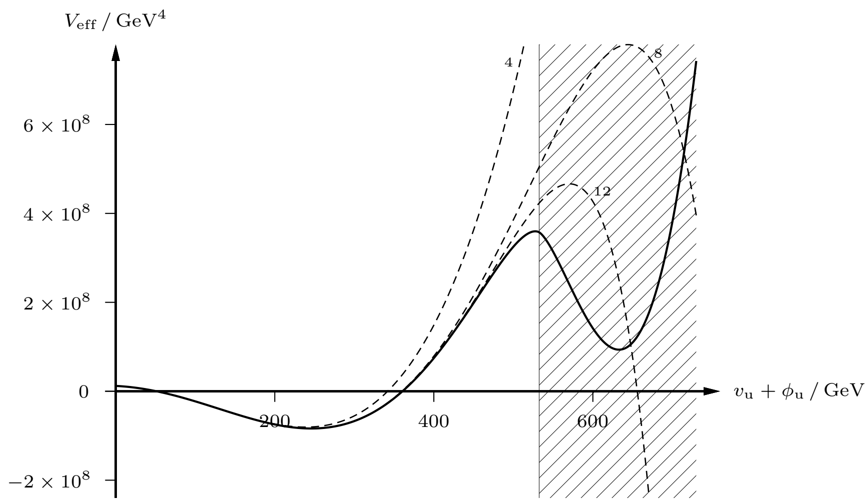

FIG. 4. The 1-loop effective potential as in Fig. 3, with μ lowered to 2.51 TeV.

from the Lagrangian. Here the field-dependent squark mass matrix of (10)—which is the second derivative of the scalar potential with respect to the sfermion fields—acquires a negative eigenvalue. If we depicted the sfermion field corresponding to this tachyonic mass eigenstate perpendicular to the drawing plane in Fig. 3, the minimum in the ϕ_{u} direction is revealed as a local maximum in the sfermion direction (*i.e.* we encounter a saddle point of the full scalar potential) and the global minimum of the scalar potential will be necessarily a charge and color breaking (CCB) vacuum. The example of Fig. 4 also shows that the existence of an imaginary part in V_{eff} alone does not directly lead to an unstable vacuum.

There exist several criteria in the literature to check whether or not the parameters lead to a CCB vacuum at tree-level. We can easily check, that we are in full agreement with the traditional criterion [**?** **?**] $A_{\text{t}}^2 < 3(M_{\tilde{Q}}^2 + M_{\tilde{t}}^2 + m_{22}^{2\,\text{tree}})$. A stronger empirical bound of $A_{\text{t}}^2 + 3\mu^2 \lesssim 7.5(M_{\tilde{Q}}^2 + M_{\tilde{t}}^2)$, which our sample point would not pass, has been suggested in [**?**]. However, this bound has been critically reviewed in the recent detailed analysis [**?**], which advocates bounds closer to the traditional measure. The criterion of [**?**] translates to $A_{\text{t}}^2 \lesssim 3.4(M_{\tilde{Q}}^2 + M_{\tilde{t}}^2) + 60 m_{22}^{2\,\text{tree}}$ in our case and is fulfilled by the parameters of Figs. 3 and 4. We are therefore safe from CCB minima of the tree-level potential.

Whenever the situation depicted in Fig. 3 occurs the corresponding MSSM parameter point is excluded. We show the excluded region of the μ–$\tan\beta$ plane in Fig. 5 for two values of the squark masses. We stress that the consideration of a single direction in the multi-dimensional space of scalar fields is not sufficient to prove the stability of the electroweak vacuum. *I.e.* to validate or discard the MSSM parameter point of Fig. 4 one would have to study all directions in the $h_{\rm u}^0$–$h_{\rm d}^0$ plane. A complete investigation further requires the study of the global minimum of the full scalar potential (including the sfermion fields) with the field-dependent sfermion masses (see (10)): As discussed above in conjunction with the second minimum of $V_{\rm eff}$, the sfermion potential is non-convex in the region with large Higgs fields with the possibility of a CCB minimum below the desired ground state of the electroweak vacuum. The determination of the global minimum of the loop-corrected full scalar potential is a formidable task and beyond the scope of this paper. An accurate determination of the contours delimiting the allowed parameter space in Fig. 5 may also require to use the renormalization-group improved two-loop result for $V_{\rm eff}$ [?].

The requirement of a stable vacuum excludes large values of $\mu \tan\beta$. The sample points studied by us also involve a large value of $A_{\rm t}$, to accommodate $m_{h^0} = 126\,\mathrm{GeV}$ through sizable stop mixing. This portion of the MSSM parameter space is of interest in flavor physics and has been widely studied: The product $A_{\rm t}\mu\tan\beta$ governs the size of the chargino contributions to $B(B \to X_s\gamma)$ [? ? ?] and the Higgs-mediated contributions to $B(B_{d,s} \to \mu^+\mu^-)$ and $B_s - \overline{B}_s$ mixing [? ? ? ? ? ? ? ? ?] grow with $A_{\rm t}$, μ and higher powers of $\tan\beta$ (see [?] for a recent study). Similar to the quark sector, flavor-changing neutral current processes in the lepton sector can be enhanced if $\mu\tan\beta$ is large [? ? ?]. Therefore the global minimum of $V_{\rm eff}$ should be checked in MSSM parameter scans of flavor observables.

IV. CONCLUSIONS

The MSSM Higgs potential receives large radiative corrections from loops with stops and (if $\tan\beta$ is large) sbottoms. Squarks which are much heavier than the Higgs bosons can be integrated out resulting in an effective Lagrangian of a two-Higgs-doublet model. The Lagrangian can be systematically improved by higher-dimensional terms suppressed by powers of $1/M^2_{\tilde{Q},\tilde{\rm t}}$. We have calculated the stop contribution to the effective self-couplings $(h_{\rm u}^{0\dagger}h_{\rm u}^0)^{d_1}(h_{\rm d}^{0\dagger}h_{\rm d}^0)^{d_2}$ of any number of neutral $h_{\rm u}^0$ or $h_{\rm d}^0$ fields at the one-loop level using an elementary diagrammatic method. Depending on the MSSM parameters entering the loop diagrams, the Higgs potential of the resulting effective Lagrangian can be unbounded from below or feature a second, unwanted minimum which is deeper than the one with $\sqrt{|h_{\rm u}^0|^2 + |h_{\rm d}^0|^2} = v = 246\,\mathrm{GeV}$. In this paper we have found that one cannot assess the question of vacuum stability from such an effective Lagrangian truncated at a finite dimension $2(d_1 + d_2)$: the critical values of $h_{\rm u,d}^0$ for which the Higgs potential drops below its value at $v = 246\,\mathrm{GeV}$ are beyond the radius of convergence of the sum over d_1, d_2.

The effective potential $V_{\rm eff}$ sums the squark-induced higher-dimensional Higgs self-couplings to all orders (without the need of any hierarchy between squark and Higgs masses) and permits the proper inclusion of top loops as well. We find that the one-loop MSSM effective potential is bounded from below but develops a second, deeper minimum, if the parameters μ, $\tan\beta$, or $A_{\rm t}$ governing the squark-Higgs couplings become too large (see Fig. 3). For two values of degenerate squark masses we have determined the region in the μ–$\tan\beta$ plane corresponding to an unstable vacuum (see Fig. 5). $A_{\rm t}$ has been chosen to reproduce the correct mass of $126\,\mathrm{GeV}$ for the lightest neutral Higgs boson, which drives $|A_{\rm t}|$ to large values. The excluded region of large $|\mu|\tan\beta$ and large $|A_{\rm t}|$ is widely studied in flavor physics, since in this region the MSSM contributions to several flavor-changing processes are large. We argue that the criterion of a global minimum of $V_{\rm eff}$ with $v = 246\,\mathrm{GeV}$ should be included in phenomenological analyses determining the allowed parameter space of the MSSM.

ACKNOWLEDGEMENTS

We are grateful for discussions on various aspects of the effective potential with L. Di Luzio, L. Mihaila, S. Pokorski, and M. Zoller. M.B. and W.G.H. acknowledge financial support of *Studienstiftung des deutschen Volkes* and the DFG-funded Research Training Group GRK 1694. G.C thanks W. Porod for useful discussions and clarifications about the `Vevacious` code. This work was supported by BMBF under grant no. 05H12VKF and the Theory-LHC-France initiative of the CNRS/IN2P3.

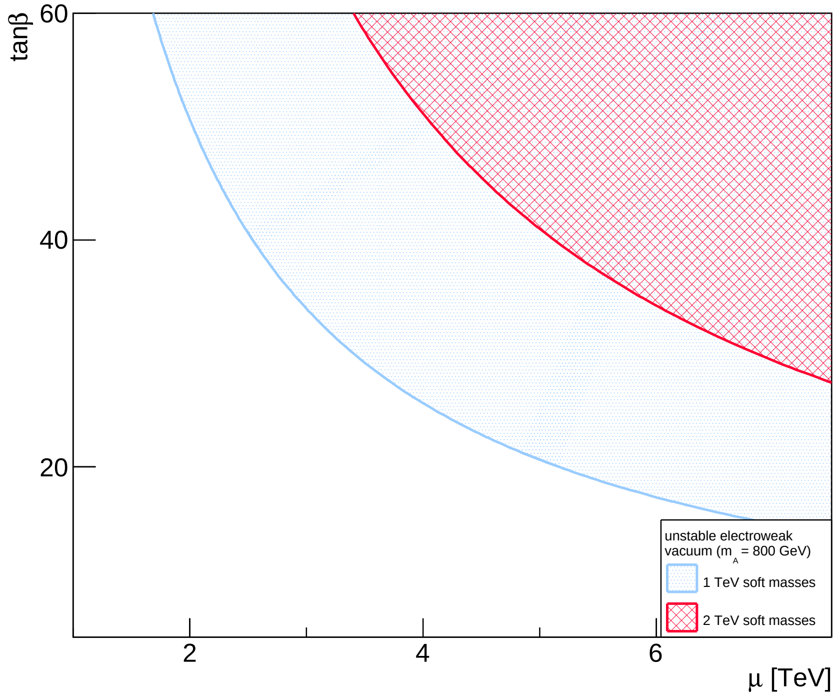

FIG. 5. Area in the μ–$\tan\beta$ plane for which $V_{\rm eff}$ develops an unwanted minimum as depicted in Fig. 3. The red, cross-hatched area corresponds to $M_{\tilde{Q}} = M_{\tilde{\rm t}} = M_{\tilde{\rm b}} = Q = 2\,\rm TeV$; the light blue area is excluded if $M_{\tilde{Q},\tilde{\rm t},\tilde{\rm b}}$ is lowered to $1\,\rm TeV$. $A_{\rm t} \simeq 1.5\,\rm TeV$ is fitted to reproduce $m_{h^0} = 126\,\rm GeV$ in both cases; $m_{A^0} = 800\,\rm GeV$ is chosen to comply with LHC search limits for $A^0 \to \tau\tau$.